

**An optimal velocity generation of a rear wheel drive tricycle  
Along a specified path**

Yasmina Bestaoui  
CEMIF, Université d'Evry, 91020 Evry, France.  
Email : [bestaoui@iup.univ-evry.fr](mailto:bestaoui@iup.univ-evry.fr)

**Abstract :** The subject of this paper is motion generation of three-wheeled vehicles, taking into account dynamics and motors' current and slew rate constraints. Dynamics are described by a nonlinear nonholonomic model. Optimal velocity is determined along a specified path. The curvature of the path is known. As an application of the proposed algorithm, velocity of the tricycle can be approximated by simple functions of the curvature.

**I. Introduction.**

While a mobile robot travels at a relatively low speed, controlling the robot with only a kinematics model may work. However, as mobile robots are designed to travel at higher speeds, dynamic modeling of these vehicles becomes increasingly important. In this paper, dynamics are integrated into motion generation, assuming that the path curvature is known. A path is specified by its geometry  $F(s) \in \mathbb{R}^2$ ,  $s \in [0, \Lambda]$ , and its motion trajectory through a function  $s(t)$ ,  $t \in [0, T]$ , where  $\Lambda$  is the length of the path and  $T$  is the total motion time. While extensive work has focused on computing the geometric path [3-9], little attention has been given to select the optimal motion. For the temporal part of the trajectory, currently most controllers use the trapezoidal speed profile. This method is suitable only for tracking straight lines. In this paper, optimal velocity is determined along a specified path with a known curvature, such as a straight line, a circle arc, a clothoid or a cubic spiral. Other paths could also be used.

**II. Modeling.**

**2.1. Description of the system.**

The mobile robot under study (see fig. 1) is made up of a rigid cart, equipped with three non deformable identical wheels, moving on a horizontal plane, with a linear velocity  $v$ .  $R_0 = \{O_0, x_0, y_0\}$  is the global reference frame while  $R_m = \{O, x_m, y_m\}$  represents the mobile frame.  $Ox_m$  is the axis of symmetry of the vehicle while  $O$  is the mid-point of the rear axle. The following distances are defined as follows :  $L$  is the distance from  $O$  to the center of the steering wheel while  $\ell$  represents the distance from  $O$  to the center of any of the rear wheels. We assume that during the motion, the plane of each wheel remains vertical and the wheel rotates about its horizontal axle whose orientation with respect to the cart is fixed for the two rear wheels and varying for the front wheel: the steering wheel. The contact of each wheel with the ground is supposed to be a point satisfying both conditions of pure rolling and non-slipping along the motion.

The configuration of the mobile robot is fully described by the following vectors [1, 2].

- Posture coordinates  $\xi = (x \ y \ \theta)^T$  for the position in the plane.

- Orientation coordinates  $\beta$  for the orientation angle of the steering wheel.

**2.2. Dynamics of a rear wheel drive tricycle.**

Two motors are controlling this conventionally driven vehicle: the first motor controls the average velocity of both rear wheels while the second motor controls the steering angle  $\beta$ . It is a rear wheel drive tricycle. The torques can be written as [1]:

$$\Gamma_1 = \frac{1}{n} (a_1 \tan^2 \beta + a_2) v + \frac{\sin \beta}{n \cos^3 \beta} a_1 v \dot{\beta} + \frac{1}{n} f_v v \quad (1)$$

$$\Gamma_2 = \frac{1}{n} I_{dw} \ddot{\beta} + \frac{1}{n} f_w \dot{\beta}$$

where the  $a_i$ 's are constant values depending on the geometric and inertial parameters of the system.

$$a_1 = \frac{n}{K} \left( \frac{I}{L^2} + \frac{2\ell^2}{r^2 L^2} I_w + \frac{I_w}{r^2} \right) \quad (2)$$

$$a_2 = \frac{n}{K} \left( M + 3 \frac{I_w}{r^2} \right)$$

with

$$M = m_p + 3m_w \quad (3)$$

$$I = I_p + m_p d^2 + 3I_{dw} + 2m_w \ell^2 + m_w L^2$$

where  $m_p$  is the mass of the platform,  $m_w$  is the mass of each wheel,  $I_p$  is the inertia moment of the platform around its center of mass,  $I_w$  is the inertia moment of one wheel around one of its diameters,  $d$  is the distance of the center of mass of the platform  $P$  to the mid-point of the rear axle  $O$ ,  $K$  is the electromechanical constant of the motor and  $n$  represents the gear ratio.

Electrical motors are very popular for driving tricycles. We focus on DC motors that are often in use. For a permanent magnet DC motor, the torque  $\Gamma$  is proportional to the armature current  $J$ . Thus actuator dynamics can be characterized in a matrix form as :

$$\Gamma = K \cdot J$$

$$U = L_t \frac{dJ}{dt} + R \cdot J + K n^{-1} (v \ \omega)^T \quad (4)$$

$$\omega = \frac{d\beta}{dt}$$

$L_t$ ,  $R$  and  $K$  are  $2 \times 2$  regular diagonal matrices representing respectively the inductance, resistance and torque constants of the actuators.  $U$  is the motor voltage vector. We assume that the transmission from the motors to the mechanism to be perfectly rigid, i.e the transmission does not suffer from backlash or flexibility.

We suppose that the inductance of the motors can be neglected. If we define the state-space variable vector  $X$

as  $X = (x \ y \ \theta \ \beta \ v \ \omega)^T$  and the control inputs as the currents produced by the system's

actuators  $(J_1 \ J_2)^T$ , then the system can be formulated as an affine nonlinear system with drift [1]:

$$\dot{X} = f_0(X) + f_1(X)J_1 + f_2(X)J_2 \quad (5)$$

with

$$f_0(X) = \begin{pmatrix} X_5 \cos X_3 \\ X_5 \sin X_3 \\ X_5 \tan X_4 / L \\ X_6 \\ -\frac{a_1 \sin X_4}{\cos^3 X_4 (a_1 \tan^2 X_4 + a_2)} X_5 X_6 \\ 0 \end{pmatrix} \quad (6)$$

$$f_1(X) = \begin{pmatrix} 0 & 0 & 0 & 0 & \frac{1}{a_1 \tan^2 X_4 + a_2} & 0 \end{pmatrix}^T \quad (7)$$

and

$$f_2(X) = \begin{pmatrix} 0 & 0 & 0 & 0 & 0 & \frac{1}{I_{dv}} \end{pmatrix}^T \quad (8)$$

On a given path, these equations of motion (5)-(8) can be written as :

$$\dot{s} = v \quad (9)$$

$$\dot{v} = g_0(s, v) + g_1(s)J_1$$

with

$$g_0(s, v) = -\frac{a_1 \ell^2 K(s) K'(s)}{a_1 \ell^2 K^2(s) + a_2} v^2 \quad (10)$$

$$g_1(s) = \frac{1}{a_1 \ell^2 K^2(s) + a_2}$$

$K$  represents the curvature and  $K'$  the derivative of the curvature versus the curvilinear abscissa  $s$ .

The current can thus be written as:

$$J_1 = A_1(s) \dot{v} + A_2(s, v) \quad (11)$$

with

$$A_1(s) = a_1 \ell^2 K^2(s) + a_2 \quad (12)$$

$$A_2(s, v) = a_1 \ell^2 K(s) K'(s) v^2$$

These equations and parameters listed above describe idealized dynamics of the system. Other effects can be identified which do not appear in eqs (1-12), including road coefficient for friction, aerodynamic forces, sliding factors, uneven road....

### III. Motion generation

#### 3.1 Problem formulation.

Designing reference trajectories is essentially an optimization problem. The minimum time trajectory generation has been solved in a number of ways, following the usual approach, i.e. taking as feasible limits purely kinematics constraints on vehicle velocity and acceleration. This bound must represent the global least upper bound of all operating accelerations so as to enable the vehicle to move under any operating conditions. This implies that the full capabilities of the vehicle cannot be utilized if the conventional approach is taken. In this paper, the case of more realistic constraints is investigated: current and slew rate constraints. In addition to current saturation, the robot also exhibits velocity saturation. This effect is due to back-EMF generation of the motors, which at high velocity, approaches the power

supply voltage of the amplifier. The inclusion of slew rate limitations smoothes the change of rate of the current.

The general problem of minimum time motion may be formulated as follows:

$$\begin{aligned} \text{Min } & t_f \\ \text{s.t. } & \text{eq. (9)} \end{aligned} \quad (13)$$

$$|J_1| < I_{\max} \quad \left| \frac{dJ_1}{dt} \right| < dI_{\max} \quad |v| < V_{\max}$$

$V_{\max}$  is the maximum velocity,  $I_{\max}$  represent the maximum of the currents and  $dI_{\max}$  the maximal slew rates. The boundary values are given by:

$$s(0) = 0; v(0) = 0; s(T) = 0; v(T) = 0. \quad (14)$$

$\Gamma_{\max}$  represent the maximum of the torques provided by

$$\text{the motors. } \Gamma_{\max} = K \cdot I_{\max} \quad (15)$$

Following [3, 9], the constraints on the currents or equivalently the torques can be transformed into constraints on the acceleration, in the phase-plane:

$$\ddot{s}_{\min}(s, v) \leq \ddot{s} \leq \ddot{s}_{\max}(s, v) \quad (16)$$

where

$$\ddot{s}_{\min}(s, v) = \begin{cases} -\Gamma_{\max} - A_2(s, v) / A_1(s) & \text{if } A_1(s) > 0 \\ -\infty & \text{if } A_1(s) = 0 \\ \Gamma_{\max} - A_2(s, v) / A_1(s) & \text{if } A_1(s) < 0 \end{cases} \quad (17)$$

$$\ddot{s}_{\max}(s, v) = \begin{cases} \Gamma_{\max} - A_2(s, v) / A_1(s) & \text{if } A_1(s) > 0 \\ +\infty & \text{if } A_1(s) = 0 \\ -\Gamma_{\max} - A_2(s, v) / A_1(s) & \text{if } A_1(s) < 0 \end{cases} \quad (18)$$

The maximum admissible velocity value is obtained

$$\text{when } \ddot{s}_{\max} = \ddot{s}_{\min}. \quad (19)$$

This defines  $v_{\max}(s)$  taking into account the mechanical limitation on velocity. Resolution of these equations uses forward and backward integration. These equations allow to construct an infeasible region in the state space  $(s, v)$ , region for which the appropriate inputs for keeping the system on the path are not available. Equations (16)-(19) are used as an analysis tool, only, verifying a posteriori that the calculated trajectories are admissible.

The next paragraph proposes a practical method of resolution when the model is supposed to be perfect.

#### 3.2 Problem resolution

According to the Pontryagin maximum principle, a time optimal solution exists in which the input switches exclusively between the maximum and minimum, possibly zero during a finite interval (when the velocity is saturated). The terminal state requirement is function of the switching interval lengths.

If we suppose that the acceleration is constant onto an interval, we can use the following approximation

$$a_k = \frac{v_k^2 - v_{k-1}^2}{2\delta} \quad \delta = s_k - s_{k-1} \quad (20)$$

In the forward integration, using equations 5 and 10

$$v_{k+1}^2 = \frac{2\delta a_1 \ell^2}{a_1 \ell^2 K^2(s) + a_2} \left( \frac{\pm J_{\max}}{a_1 \ell^2} - \frac{a_1 \ell^2 K^2(s) + a_2}{2\delta a_1 \ell^2} K(s)K'(s)v_k^2 \right) \quad (21)$$

The actual velocity depends on the past velocity, the path curvature and its derivative, the motor current and the mobile robot parameters.

When the equality of velocities (eq 21) computed with forward and backward integration is obtained, this is considered as the switching time. Accelerations are obtained with eq. 9.

For each  $s$ , the path curvature and its derivative are known. The characteristic of this motion generation technique is that the curvilinear abscissa  $s$  is the variable, while the time  $t$  is a function of  $s$ .

Other sub-optimal methods can be used such as polynomial functions, sinusoidal curves... to provide a higher degree of continuity.

#### IV. Numerical examples

##### 4.1. Robot characteristics.

Many simulations were performed with a mobile robot that characteristics are:

$I_p=5.5\text{Kg}\cdot\text{m}^2$ ;  $I_w=I_{dw}=0.24\text{Kg}\cdot\text{m}^2$ ;  $m_p=10\text{Kg}$ ;  $m_w=1\text{Kg}$ ;  $r=0.1\text{m}$ ;  $l=0.2\text{m}$ ;  $d=0.5\text{m}$ ;  $L=1\text{m}$ .

Both motors are identical:

$K=1.5\text{Nm/A}$ ;  $n=1$ ;  $I_{\max}=15\text{A}$ ;  $dI_{\max}=15000\text{A}$ ;  $v_{\max}=4\text{m/s}$ .

##### 4.2. Simulation results.

The length of the path is 4m. The initial conditions are  $x(0)=y(0)=\theta(0)=0$ . The algorithm stops when the precision is less than 0.01. The simulations are performed using MATLAB software.

In this paper, four examples are presented

For the straight line (fig. 2),  $K(s)=0$ ;

For the circle (fig. 3),  $K(s)=1$ ;

For the clothoid (fig. 4),  $K(s)=s$ ;

For the cubic spiral (fig. 5),  $K(s)=s^2$

Each figure represents the velocity, acceleration, current, orientation, curvature and evolution of the time with respect to  $s$ , then the path ( $x$ - $y$ ) is presented and finally current versus time  $t$ .

Although it may seem that the slope of the current is infinite, it is not. The slew rate limitation is considered.

##### 4.3. Application: Approximation of the velocity as a simple function of the curvature.

As known from everyday experience, velocity depends on the curvature of the road. Higher is the curvature, lower is the velocity. In this paragraph, three different kind of functions are compared with the solution of integration of the differential equations (9). The following functions are used:

$$v = \alpha \exp(-\beta|K(s)|)(\Lambda - s) \quad (22)$$

$$v = \frac{(\Lambda - s)}{|K| + \beta} \quad (23)$$

$$v = \left( \Lambda - s \sqrt{|K|^2 + \beta} \right) \quad (24)$$

where  $\alpha$  and  $\beta$  are parameters depending on the characteristics of the path and the vehicle.

Figures 6 and 7 show the applicability of these approximation when the velocity obtained after resolution

of the differential equations and the three approximations (22), (23), (24) are plotted versus curvature.

These approximations can be generalized in the path generation and the path tracking of any tricycle.

#### V. Conclusions

In specifying a trajectory, the physical limits of the system must be considered. This paper presents a method for generating smooth motion for robotic vehicles on a given path when kinematics and dynamics constraints are taken into account. We are interested in finding a trajectory that is optimal in motion time subject to velocity and current constraints.

For motors, the voltage is limited. If the inductance of the motors cannot be neglected, then combining motor equations with dynamics leads to a set of third order equations. Our future work will introduce voltage constraints into motion generation, with non negligible inductance.

Although DC motors have been considered, other actuators such as AC machines present the same kind of constraints on both the current and voltage.

This motion generation algorithm is applied to a rear wheel drive tricycle. It can be easily generated to a front wheel drive, a differentially steered or any other kind of mobile robot.

For kinematics models, the stabilization problem has essentially been solved with two types of control laws:

- time-varying piecewise continuous control.
- Time-varying continuous control.

An analogous study must be made for vehicles represented by their kino-dynamics models.

Interesting applications of Hamiltonian methods, such as the energy-momentum method (for determining nonlinear stability) and bifurcation of Hamiltonian systems with symmetry (for uncovering non trivial branches of new solutions when system parameters such as friction coefficients are varied) are also another perspective. Other studies can be conducted about sliding, deformability or flexibility of the wheels.

#### VI. References

- [1] Y. Bestaoui 'Dynamics of a three-wheeled vehicle driven by DC motors' ASME-IMECE Symposium on Innovations in Vehicle design and Development, Nashville, TN, Nov. 1999.
- [2] C. Canudas, B. Siciliano editors ' Theory of robot control' Springer-Verlag, 1996.
- [3] O. Dahl, L. Nielsen 'Torque-limited path following by on-line trajectory time scaling' IEEE Trans. On Robotics and Automation, vol 6, #5, pp. 554-561, 1990.
- [4] H. Hu, M. Brady, P. Probert ' Trajectory planning and optimal tracking for an industrial mobile robot' SPIE, Boston, Ma, vol. 2058, 1993, pp. 152-163.
- [5] Y. Kanayama, B. I. Hartmann 'Smooth local path planning for autonomous vehicles' Autonomous Robot Vehicles, I. J. Cox, G. T. Wilfong ed., Springer-Verlag, 1990, pp. 62-67.
- [6] V. Munoz, A. Ollero, M. Prado, A. Simon 'Mobile robot trajectory planning with dynamic and kinematic constraints' IEEE Int. Conf. On Robotics and Automation, 1994, pp. 2802-2807.
- [7] D. B. Reister, F. G. Pin 'Time-optimal trajectories for mobile robots with two

independently driven wheels' International Journal of Robotics Research, vol. 13, #1, 1994, pp. 38-54.

- [8] N. Sadegh, B. Driessen 'Minimum time trajectory learning' American Control Conference, 1995, Seattle, WA, pp. 1350-1354.
- [9] Z. Shiller, H. H. Lu 'Computation of path constrained time optimal motions, with dynamic singularities' Journal of dynamic systems, measurement and control, vol. 114, pp. 34-41, 1992.

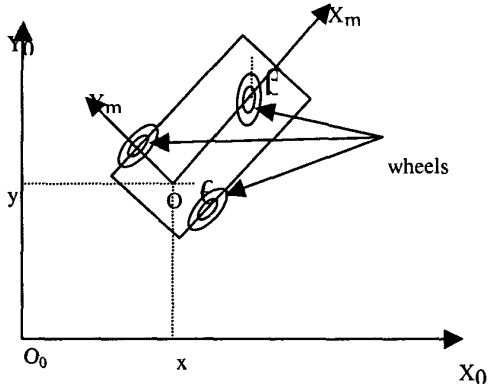


Figure 1

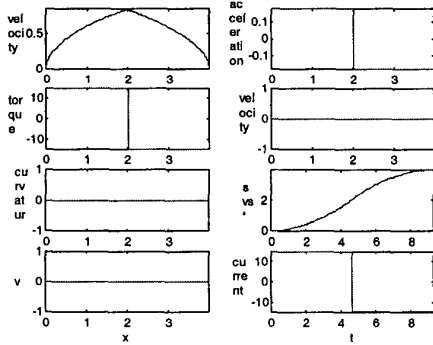


Figure 2

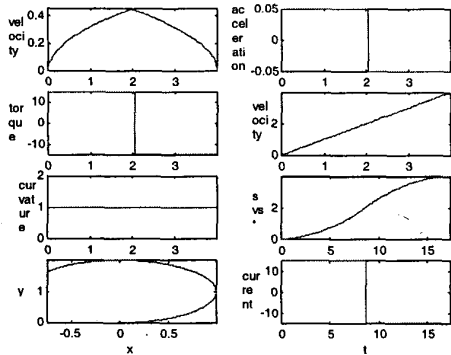


Figure 3

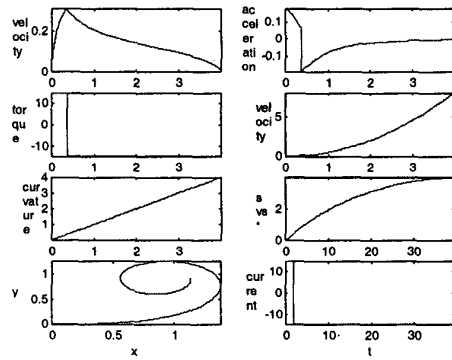


Figure 4

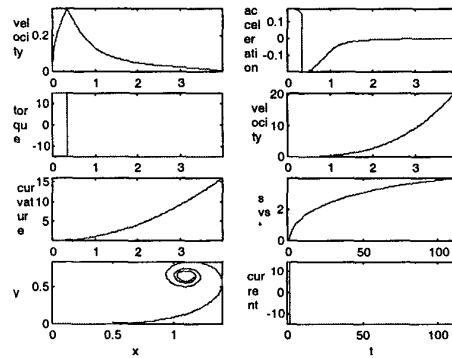


Figure 5

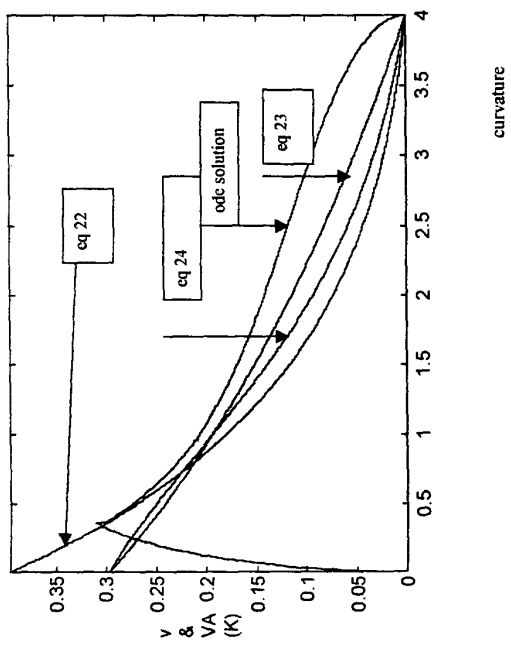


Figure 6

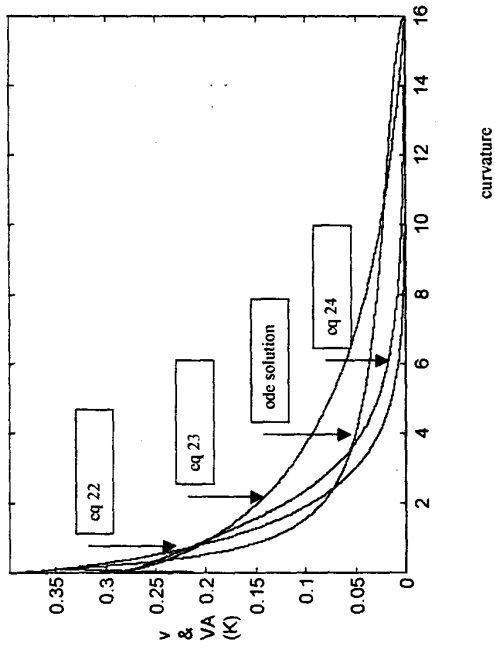


figure 7